

# Long roughness measurements – Analysis and possible protocol

A. Bracciali

*Dipartimento di Meccanica e Tecnologie Industriali, University of Florence, via Santa Marta 3,  
50139 Firenze, Italy*

*Tel: +39 347 2429240, Fax: +39 055 4796400, E-mail: bracciali@ing.unifi.it*

## Abstract

Long rail roughness measurements are provided by draft standards on noise emission and are a common practice but no protocol is currently available to take advantage of the great amount of information made available by them. The paper reviews current standards and procedure for short measuring equipment and extend them, proposing a new analysis procedure for long measurements. Practical examples are illustrated, showing the applicability of the protocol and its efficiency.

## 1. Introduction

Rail roughness is recognised to be a critical parameter in the rolling noise generation mechanism, and its measurement and assessment is critical to ensure the validity of the measurement of the noise pressure levels measured during trains pass-by.

Such measurements can be used for different purposes, like estimation of the annoyance level during a given period of time (day, evening, night), type testing of new vehicles, comparison of different trains in the same site or comparison of different sites with the same train.

In all these activities, wheel and rail (or, more generally, the entire track) behaviour are critical but normally quite out of the possibility of control by the sound engineer. Some modifications can be done to limited track sections by changing the rail pads with a type more suitable for noise purposes, but as the high stiffness normally requested to obtain good track vibroacoustic properties are very high and can lead to other problems, the only parameter on which the specialist can really act is the rail roughness.

Current standards, discussed later, do not cover completely the possibilities of existing equipment in terms of rail roughness measurement and analysis. This paper proposes a methodology for analysing very long roughness measurements obtained with a trolley. It is shown that the statistical quality of the results is extremely high, and some guidelines to assess the quality of a site are proposed which complement the standards in force.

## 2. Current standards on rail roughness measurements

### 2.1. Standards description and comparison

The standard in force for rail vehicles is still ISO 3095:1975, even if the revision process of EN ISO 3095 is completed and it should be published during 2004. Nevertheless, other official documents refer to prEN ISO 3095:2001 draft version, and some further work is extending the range of validity of the same standards. It seems worth therefore to briefly summarize the protocol stated in the various ISO standard versions and their modifications:

- *The prEN ISO 3095:2001 draft standard.* This draft standard [1] was released in January 2001 and circulated between CEN and ISO members for comments. Although deeply modified later, it is still referenced by the TSI-HS-RS (see later) and is briefly reported here. Roughness is described in Annex D that defines a track reference section long  $4r$ , where  $r$  is the distance of the measuring microphone from the track axis (Fig. 1). Rail roughness should be measured over the six cross sections indicated in Fig. 1. Each section is at least 1 m long and one or three parallel lines must be measured if the “running band” width is respectively smaller or larger than 10 mm. Roughness spectra of all sections must be averaged and compared with the limits spectrum shown in Fig. 8 at the end of the paper. The comparison allows some overcoming of this spectrum, not described here. The wavelength range of comparison is between 10 mm and 80 mm (Note: ref. [1] uses cm as a unit of length).

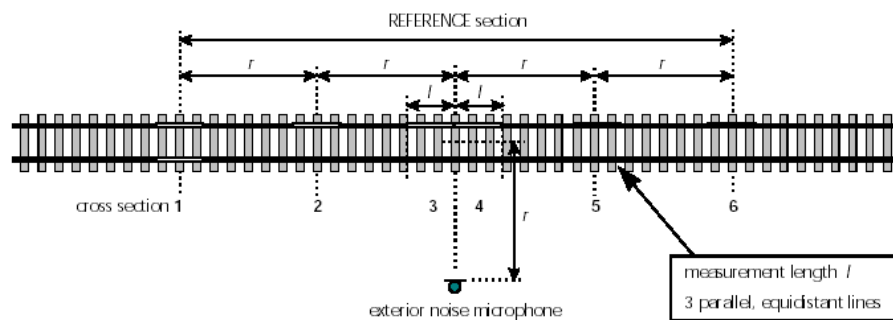


Figure. 1. Rail roughness measurement protocol as described in [1].

- *The TSI-HS-RS standard.* Technical Specification for Interoperability – High Speed – Rolling Stock [2] refers directly to the prEN ISO 3095:2001 Draft to perform rail roughness measurements. A different limit spectrum (Fig. 8) is given by using an explicit equation. The wavelength range of validity is between 200 mm and 5 mm (Note: ref. [2] uses m as a unit of length).
- *Further studies by AEIF.* Although the discussion of the results from AEIF (European Association for Railway Interoperability) lies outside the scope of this paper, it is worth to mention that other limits were proposed during the NOEMIE (NOise Emission Measurements for high speed Interoperability in Europe) activities [3], aiming at a further reduction of the uncertainty in the measured noise levels. This limit was called ATSI (Alternative TSI) limit (Fig. 2); after extensive experimental campaigns, this more demanding limit seems to be relaxed and brought back to TSI limit for high speed trains, while further investigation is needed for conventional speed. The interested reader is referred to AEIF for further details.
- *The EN ISO 3095:2004 standard.* The Annex A of the final version of the standard on external noise [4] introduced the concept of long measurements. Subsection A.2.2.1 states that rail roughness shall be measured on the whole reference section, although measurements with equipment capable to measure only limited lengths  $l$ , with a minimum of  $l=1$  m, are accepted. Nevertheless, the valid upper wavelength limit depends also on the measured length  $l$ ; for example,  $l=1$  m produces acceptable results only up to wavelengths around 0.100 m. The remaining part of the Annex describes only the processing of limited length measurements with the protocol indicated in the 2001 version, without any indication on how to perform long measurements processing.

All the described standards compare the current average spectrum with a limit spectrum whose values in dB ref. 1  $\mu\text{m}$  are given (as in the case of TSI) or can be described (ISO 3095, ATSI) as a logarithmic function of the centre band wavelength as

$$L_{rough}(\lambda) = a + b \log_{10} \left( \frac{\lambda_0}{\lambda} \right) \quad (1)$$

where  $a=4$  and  $b=-6$  for TSI,  $a=27.176$  and  $b=-18.419$  for ISO 3095 (down to 10 mm),  $a=25.166$  and  $b=-20.238$  for ATSI (down to 10 mm) and  $\lambda_0=1$  m in all cases. The curves are shown in Fig. 8 hereinafter.

### 3. Limitation of current standards

#### 3.1. Introduction

The definition of the limits shown in the previous paragraph comes from the experience gained during years of measurements. It seems therefore clear that rail roughness is a broad band phenomenon, and the appearance of clear sinusoidal longitudinal patterns ('corrugation') is negative and must be avoided as much as possible. Normally corrugation appears on the low rail in tight curves, but numerous cases in tangent track are daily experience in several railway administrations.

The case of corrugation is not considered here, and the attention will be focused on the random-like nature of rail roughness. The numerical analysis of random signals can be performed in two distinct but strictly related techniques:

- by finding narrow-band spectral properties using Fourier analysis, or
- by finding constant percentage band spectral properties using parallel (digital) filtering.

In ref. [4] the author has carried out a critical analysis on the limitation of the standards available at that time, including numerous considerations on equipment resolution and the possible pitfalls in signal processing. Some conclusions are repeated here to justify the approach adopted in the following.

#### 3.2. Reference track sampling related limitations

By using the ISO 3095 protocol, only 6 sections over the entire reference sections are measured, i.e. 6% of the rails for the classical case of measurements taken at 25 m from the track axis. Without proving that the remaining (unmeasured) portions of the track are affected by the same rail roughness, the hypothesis of uniform roughness must be done. Unfortunately it is often the case, as for example shown by long roughness measurements described in [6], that even visually similar track sections can have differences of some dB in some roughness spectrum bands. It is therefore necessary to acquire a much greater number of samples to get a correct statistical representation of the rail roughness phenomenon.

#### 3.3. Uncertainties due to limited measuring length

If the measuring length is limited the estimated spectrum is affected by a statistical uncertainty which depends on the wavelength considered. Even if the uncertainty analysis is easier working in the space (time) domain by using the theory of errors applied to digital filters, there is no difference in principle between using digital filters and FFT procedures.

To have a correct estimation of the output of a band-pass filter of amplitude  $B$  when the input is a pure sine wave it is necessary that [5]

$$BT = K \geq 1 \quad (2)$$

where  $T$  is the time of acquisition.

Dealing with roughness measurements, time is substituted by space. Working in the space domain, let us indicate with  $B_s$  the filter amplitude (difference of the inverse wavelengths) and change  $T$  with  $L$ , i.e. the length of the measurement. For the general case of a random input, the approximate ratio  $\varepsilon$  between the filter output RMS standard deviation  $\sigma$  and its RMS value  $\mu$  is given by

$$\frac{\sigma}{\mu} = \varepsilon = \frac{1}{2\sqrt{B_s L}} = \frac{1}{2\sqrt{K}} \quad (\text{for } K > 10) \quad (3)$$

or, expressed in dB for any value of  $\mu$ ,

$$\varepsilon_{dB} = 20 \log_{10} \left( \frac{\mu \pm \sigma}{\mu} \right) = 20 \log_{10} (1 \pm \varepsilon) = 20 \frac{\ln(1 \pm \varepsilon)}{\ln 10} = 8.69 \ln(1 \pm \varepsilon) \quad (4)$$

Supposing to use  $B_s L = K$  values such that  $\varepsilon \ll 1$ , Equation (4) simplifies to

$$\varepsilon_{dB,app} = 8.69(\pm \varepsilon) = \pm \frac{8.69}{2\sqrt{K}} = \pm \frac{4.35}{\sqrt{K}} \quad (5)$$

It is worth to note that the corrugation signal is neither a pink noise nor a white random Gaussian noise as the constant percentage band PSD decreases at smaller wavelength centres (i.e. increasing the frequency), but its random nature approximately remains in each band as it can be considered, as usual, independent from the others.

Two approaches can be used when making a measurement: an approach by keeping  $K$  (and therefore the error  $\varepsilon$ ) constant by changing the length of measurement for each band or, more commonly, by keeping  $L$  constant obtaining therefore a different error  $\varepsilon$  in each wavelength range. To compare the two approaches some calculations are shown in Table 1 for the following cases:

- a measurement with  $L=1.2$  m independently from the wavelength, for which the value of  $K$  and the error  $\varepsilon$  is computed in percentage and in dB for each 1/3 octave wavelength band;
- a similar analysis for  $L=100$  m;
- a measurement with  $K=20$ , for which the required length in each wavelength band is calculated while the errors remain (obviously) constant around 1 dB.

It is clear that the errors in the  $L=1.2$  m case are unacceptable even for wavelengths  $\lambda_c=0.1$  m (the relative statistical error is 30% of the average RMS) while the  $L=100$  m gives reasonable results in the whole selected wavelength range. From the analysis of this table it should appear clearly that the measurement of short segments can lead to erroneous conclusions. The use of equipment capable to measure only up to 1 m or 1.5 m allows to obtain longer records only by pasting several records, but this procedure can be slowly and tricky, as the joining phase is not trivial. In this respect, the use of a virtually unlimited length measurement is decisively superior.

TABLE 1

*Statistical errors for the 1/3 octave bands centred from 0.01 m to 0.1 m.*

$\lambda_c$ [m]	$f_s$ [m <sup>-1</sup> ]	$B_s$ [m <sup>-1</sup> ]	$K_{L=1.2\text{ m}}$	$\varepsilon_{L=1.2\text{ m}}$ [%]	$\varepsilon_{L=1.2\text{ m}}$ [dB]	$K_{L=100\text{ m}}$	$\varepsilon_{\%L=100\text{ m}}$ [%]	$\varepsilon_{L=100\text{ m}}$ [dB]	$L_{K=20}$ [m]	$\varepsilon_{K=20}$ [%]	$\varepsilon_{K=20}$ [dB]
0.1000	10	2.32	2.78	30.0	2.61	232	3.29	0.286	8.64	11.2	0.973
0.0800	12.5	2.89	3.47	26.8	2.33	289	2.94	0.256	6.91	11.2	0.973
0.0630	15.9	3.68	4.41	23.8	2.07	368	2.61	0.227	5.44	11.2	0.973
0.0500	20	4.63	5.56	21.2	1.85	463	2.32	0.202	4.32	11.2	0.973
0.0400	25	5.79	6.95	19.0	1.65	579	2.08	0.181	3.45	11.2	0.973
0.0315	31.7	7.35	8.82	16.8	1.46	735	1.84	0.160	2.72	11.2	0.973
0.0250	40	9.26	11.1	15.0	1.30	926	1.64	0.143	2.16	11.2	0.973
0.0200	50	11.6	13.9	13.4	1.17	1160	1.47	0.128	1.73	11.2	0.973
0.0160	62.5	14.5	17.4	12.0	1.04	1450	1.31	0.114	1.38	11.2	0.973
0.0125	80	18.5	22.2	10.6	0.923	1850	1.16	0.101	1.08	11.2	0.973
0.0100	100	23.2	27.8	9.49	0.825	2320	1.04	0.090	0.86	11.2	0.973

### 3.4. Pits and spikes processing

Measurements can be affected by local irregularities, commonly known as ‘pits’ and ‘spikes’. The approach normally used for limited length measurements is to artificially remove these irregularities by not yet standardised procedures. Still recently a benchmark on the same raw data by different subjects has shown [7] that the processing procedure has a very large influence on the final spectrum.

Some questions that can not be answered with limited length measurements are the following: how many sections are affected by pits & spikes? Are they so numerous that the reference track can not be accepted or the appears just in the measured section? Having the possibility of shifting the microphone by 1 or 2 m, other pits & spikes would be found or instead a track without these local defects?

It is the author’s opinion that the entire subject of pits & spikes processing must be superseded by a statistical analysis of the number of irregularities in the entire track.

## 4. The long roughness measurement protocol

### 4.1. An indicator of local irregularities

Fundamental to obtain valid long roughness measurements is the availability of an equipment capable of measuring rapidly and with the required precision long portions of a rail. Other desired features are the portability of the equipment and the possibility to be operated by one person. For the purpose of this work a CAT (Corrugation Analysis Trolley) was used. A thorough description of the equipment can be found in [8].

When long measurements (‘traces’) are available, a suitable procedure is needed to avoid a time-consuming visual check of the entire trace. When splitting a trace in consecutive ‘sections’, it is quite easy to find pits or spikes in some of them. Local irregularities have two common features: they increase the mean energy (RMS) of the defective section compared to non defective sections and they give rise to high crest factors. Several attempts have been done to identify a sufficiently robust indicator capable to detect local irregularities in signals of different RMS: it is clear that a 1

$\mu\text{m}$  peak in a signal with  $0.1 \mu\text{m}$  RMS is much less important than a peak of  $100 \mu\text{m}$  in a signal with  $10 \mu\text{m}$  RMS, even if the crest factor remains the same.

The indicator proposed here is a combination of the standard deviation (=RMS) and the kurtosis of the section. Kurtosis, that is the fourth statistical moment of a given signal, is widely used in machinery diagnostics, particularly for rolling element bearings. Because the fourth power is involved, the value of kurtosis is weighted towards the values in the tails of the probability density distribution – i.e. it is related to the spread in the distribution. The value of kurtosis for a Gaussian distribution is 3. A higher kurtosis value indicates that there is a larger spread of higher signal values that would generally be the case for a Gaussian distribution. The kurtosis of a signal is very useful for detecting the presence of an impulse within the signal [5].

For continuous and sampled discrete signals in the time domain the kurtosis is defined respectively as

$$kurtosis(X) = \frac{E[x^4]}{\sigma^4} = \frac{1}{\sigma^4} \int_{-\infty}^{+\infty} x^4 p(x) dx = \frac{1}{\sigma^4 T} \int_0^T x^4 dt ; kurtosis(X) = \frac{\frac{1}{n} \sum_{i=1}^n (x_i - \mu)^4}{\left( \frac{1}{n} \sum_{i=1}^n (x_i - \mu)^2 \right)^2} \quad (6),(6')$$

where the quantity in Equation (6') is normally referred to 'scaled' or 'normalized' kurtosis. The Defect Indicator Factor (*DIF*) indicator proposed uses the 'unscaled' kurtosis applied over a short section vector *X*:

$$DIF = 20 * \log_{10}(kurtosis(X) * std(X)^4) \quad (7)$$

where both *kurtosis* (scaled) and *std* are standard MATLAB functions. If the section is  $100 \text{ mm}$  long, the spatial sampling is  $1 \text{ mm}$  and the amplitude of *X* is expressed in  $\mu\text{m}$ , it was found that the application of Equation (7) leads to acceptable results in a large variety of practical cases. A section can be considered defective if  $DIF > 40 \text{ dB}$ .

Applications of this criterion immediately finds defective sections in long measurements and gives also a numerical indication of the severity of a local surface irregularity issuing a list of defective sections. A visual check can be done to confirm the measurement outputs or, if needed, to repeat the measurement.

If long enough, the longest non defective section of the railhead can then be used to estimate the roughness spectrum. If this information is considered not sufficient, the filtering process described later can give a different option to estimate spectral properties with even lower statistical uncertainty.

#### 4.2. Perfect filtering of long traces

Typically [9, 10], the calculation of the roughness spectrum from a 'short' ( $\approx 1 \text{ m}$ ) measurement is performed through several steps: a) windowing the trace with a Tukey (cosine-tapered) window to reduce leakage problems, b) performing an FFT to evaluate the narrow-band spectrum and c) grouping the bands (adding the energy) to fill the 1/3-octave bands required by the standard. The use of a Tukey window, which has not the best leakage properties, is due to the fact that any windowing process reduces the useful signal length. Resolution at lower spatial frequencies (longer wavelengths) is poor (few spectral lines to be added) but this is not due to any intrinsic limit of Fourier analysis but to the small number of samples which results in a low frequency resolution. Obviously this is the same problem described in section 3.3 seen from the FFT point of view; all

considerations reported there are valid also for this case.

The use of long traces allows a different usage of the FFT analysis. In the hypothesis of traces 100 to 400 m long (100.000 to 400.000 samples), it is clear that frequency resolution increases dramatically and there is no problem of grouping bands even at the longer wavelengths. On the contrary, it is also clear that the energy in a 1/3-octave band of the entire signal is meaningless, as it may contain subsections of different roughness and local irregularities. Nevertheless the availability of an extremely fine narrow band spectrum allows the use of the so-called ‘perfect filtering’ procedure which consists of 5 steps:

- a) application of a Tukey window with a very low taper ratio value (*tukeywin* MATLAB command), such that only the first and last 2000 to 5000 samples are affected;
- b) FFT calculation;
- c) zeroing spectral lines from step b) which fall outside the band-pass region of interest;
- d) inverse FFT calculation;
- e) repeat from step c) until all 1/3-octave bands are considered.

Perfect filtering results in a filter with zero ripple in the band-pass region, infinite roll off and no phase shift of spectral components. No other filter, either digital or analogue, has these properties. Obviously the application of a Tukey window reduces the validity of the end samples; to prevent such problems the measurement length should exceed by approximately 5 m (5000 samples) the trace length that is going to be analysed. With the CAT equipment this does not represent a problem at all.

#### 4.3. Roughness spectrum calculation

Once perfect filtering was applied, a number of 1/3-octave band filtered traces are available. From these signals it is possible to remove defective sections previously identified and to paste the new traces into shorter traces. The straightforward calculation of spectral components reduces therefore to the calculation of RMS for desired slices of the traces. Note that the RMS calculated does not contain any filtering and therefore pasting remaining sections does not lead to any irregularity due to sudden steps between remaining sections.

As the number of 100 mm-long defective sections found applying the  $DIF > 40$  dB criterion is normally below 5%, the remaining 95% of roughness traces are available for spectrum estimation. Incidentally, this is almost exactly the opposite of the current ISO protocol where only 6% of the reference track is measured. The statistical reliability of the process is extremely high also for long wavelengths; as an example, for the 1/3-octave wavelength band centred at 0.5 m, if 95 m are available (5% local irregularities over 100 m), the statistical uncertainty calculated using (5) is  $\varepsilon_{dB,app} \pm 0.65$  dB. These uncertainty values are not reachable by fixed-length measuring equipment.

#### 4.4. Proposal for further reference section approval criteria

The considerations arising from the method described may impact strongly the future work of standardisation institutions. They can be summarised as follows:

- a) The averaging process of all traces indicated in the ISO standard ignores the fundamental fact that noise measured by a microphone depends on the source strength *and* on the distance, once that the propagation law and directivity properties are known. Currently, a very rough section far away from the microphone can lead to the rejection of a test site,

even if its importance is clearly low. Procedures to take into account the geometry of the measurement site, like the one described in [4] which lowers the importance of distant portions of the rail, should be implemented in future standards.

- b) Sometimes the microphone position may be shifted by several metres. A criterion to put the microphone in the most uniform region (see again [4]) should be considered. It leads to considerable reduction of the effects of differences in the different sections and can reduce also the effects of pits & spikes on noise.
- c) In current standards the average spectrum from different traces is simply averaged. If the traces are highly (perfectly) correlated this means that all possible wheel-rail contact points have the same roughness pattern [11]. If the traces are not correlated or if the wheel is laterally shifted, as in curves or for incorrect bogie attitude, noise can vary by several dB [12]. The information on the contact point location is fundamental but it is not available during roughness measurement. This point requires further investigations, but probably the measurement of just one long trace centred in the running band could be sufficient as no other hypothesis has stronger foundations.
- d) Long measurements should be divided in standard length sections, for example 5 m long. The spectra from these sections should be averaged giving information on how roughness varies along the reference track. A limit on standard deviation should be given.
- e) The final roughness spectrum at the previous point should indicate the statistical reliability calculated with Equation (5). Note that a criterion on the amplitude of this parameter is indirectly a criterion on the measurement length.
- f) As long as railway noise depends on the *combined* roughness, it would be opportune to filter the roughness with a contact patch filter. Unfortunately the actual shape (transverse profile) of wheels passing over the track is not known; nevertheless a first approximation filtering should be considered. This point requires further investigations.

## 5. An example of application of the protocol

### 5.1. Irregularity analysis of a trace measured on a high-speed track

Measurements shown here are taken on a track of a railway line specialised for high-speed traffic. Track type is classical, with monobloc concrete sleepers, elastic clips, rail pads, ballast. No information are available about grinding or traffic passed over the track after grinding. Six 200 m-long traces were acquired. A track description and a picture of the rail surface are shown in Fig. 2.

After extensive analysis, it was observed that *DIF* gives the best results on roughness traces filtered in the 10÷200 mm wavelength range. This filtering is used *only* for defect detection purposes and has no effect on RMS spectra. After filtering, the first and the last 2 m have been removed to eliminate the initial effect of both the CAT equipment and of the filter behaviour. The remaining 196 m-long signal has been divided in 100 mm-long sections, numbered consecutively from 1 to 1960. Even if both *kurtosis* and *std* MATLAB functions remove the mean  $\mu$  of the signal, each section has been corrected before the application of the *DIF* criterion by using the *detrend* MATLAB function which removes linear trends.

The application of the *DIF* criterion proved to be effective, finding short and long defects, weighing correctly both the energy and the irregularity of the signal in the section. The *DIF* value also gives a degree of importance of the defect, opening the possibility to selective check of the rail surface only in those points where *DIF* is particularly high. Some example of detection of defects with different characteristics are shown in Fig. 3.

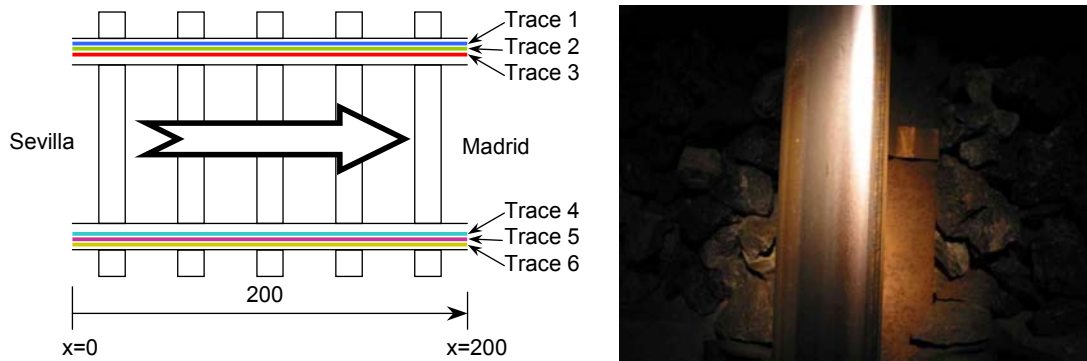


Figure 2. Traces numbering and rail aspect. Note the extreme width of the running band, which covers almost all the railhead

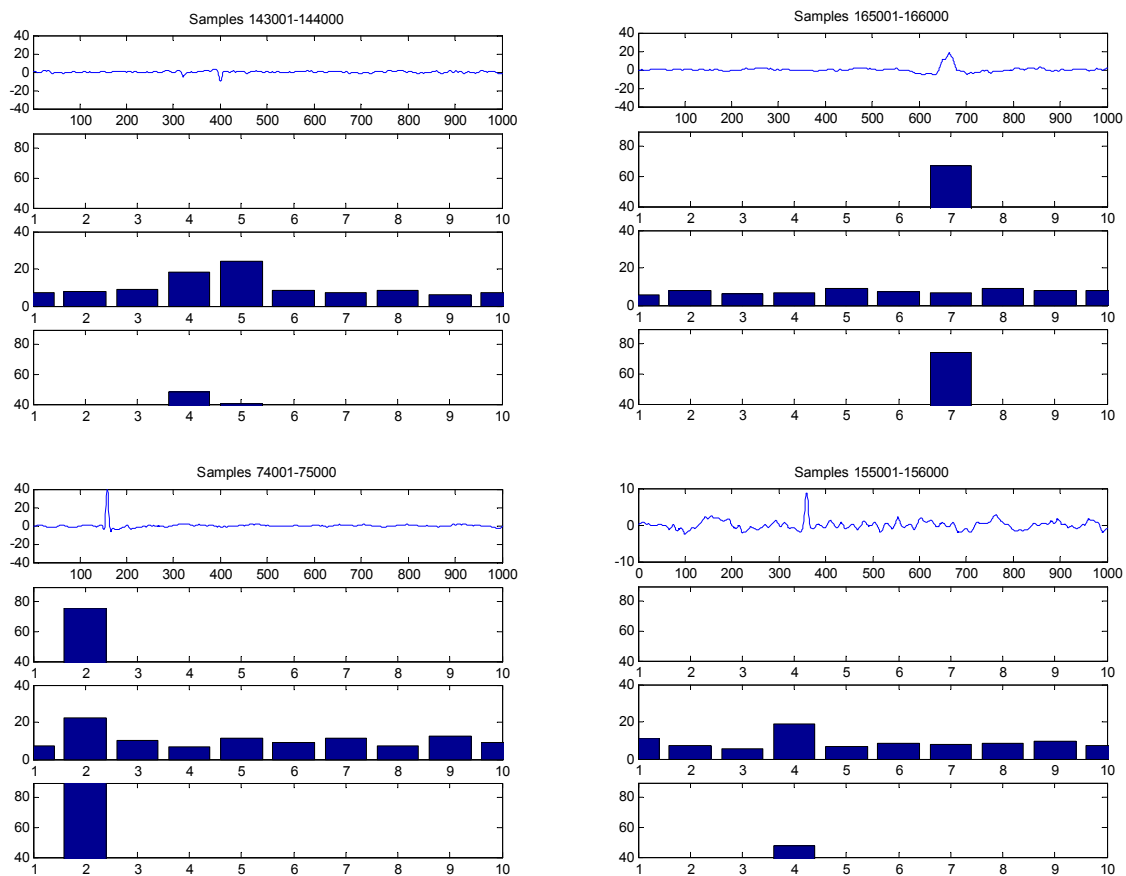


Figure 3. Examples of application to Trace 2 of pits & spikes finding procedure. Upper left: detection of a small pit with low energy but high kurtosis. Upper right: detection of a large spike with high energy and low kurtosis. Lower left and right: detection of short peaks of similar shape but different amplitude. Row plots are: signal filtered in the 10÷200 mm wavelength range,  $std^d$  in dB, scaled *kurtosis* in dB, *DIF*.

A total of 48 defective sections over 1960 ( $\approx 2.5\%$ ) were found. After looking at the defects position it is possible to find the railhead consecutive portions which are not affected by defects (Table 2). It can be seen that the longest non defective portion is 27.6 m long, starting at 28.8 m and ending at 56.3 m. This is certainly a place where a microphone could be placed. It is interesting to note that there are 10 portions longer than 5 m without defects.

TABLE 2

Identification of contiguous non defective portions for Trace 2. CS= number of consecutive sections, BS=beginning section, ES=ending section. Section length in m is given by CS/10

CS	BS	ES	CS	BS	ES	CS	BS	ES	CS	BS	ES
276	288	563	53	1706	1758	26	716	741	11	191	201
186	743	928	45	1207	1251	25	1449	1473	10	1694	1703
183	1	183	44	997	1040	25	566	590	10	203	212
164	1042	1205	44	952	995	24	1633	1656	6	1658	1663
139	1295	1433	41	1253	1293	23	692	714	5	946	950
82	592	673	35	1838	1872	15	675	689	2	930	931
77	1760	1836	34	1569	1602	13	1555	1567	2	188	189
77	1477	1553	26	1666	1691	12	1436	1447	1	186	186
73	214	286	26	1605	1630	11	933	943			

### 5.2. Irregularity analysis of all six traces

Following the ISO protocol, it is certainly interesting to look for track portions where *none* of the traces has a defect. Repeating the procedure for all traces and combining the results, the portions shown in Table 3 were found. Clearly the longest non defective portion is shorter than for the single trace; in any case it is still possible to find five portions longer than 5 m.

It is interesting to see how clusters of defects are present on each rail, showing that when a defect is present on a trace it is often present also on the other traces on the same rail (Fig. 4).

TABLE 3

Identification of contiguous non defective portions for all traces. CS= number of consecutive sections, BS=beginning section, ES=ending section. Section length in m is given by CS/10

CS	BS	ES									
86	367	452	38	33	70	23	1319	1341	19	863	881
56	592	647	33	254	286	23	1271	1293	18	1787	1804
53	88	140	30	1511	1540	23	692	714	18	329	346
52	1347	1398	27	1207	1233	23	305	327	16	288	303
51	468	518	27	226	252	22	1838	1859	16	160	175
48	814	861	26	1760	1785	22	1737	1758	15	1605	1619
47	1877	1923	25	1706	1730	21	1069	1089	15	1455	1469
45	746	790	25	958	982	21	792	812	15	1416	1430
41	1127	1167	24	567	590	21	721	741	15	1183	1197

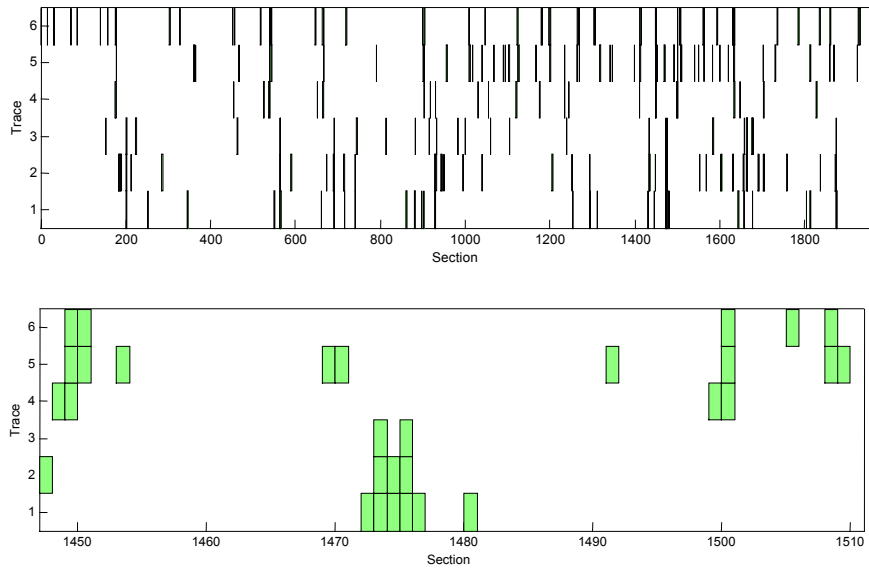


Figure 4. Defects found in all traces (top). Close-up showing defect clustering on left rail (traces 1-3) and on right rail (traces 4-6)

### 5.3. Spectral analysis of Trace 2

Raw Trace 2 was filtered with the perfect filtering procedure described at section 4.3. After filtering, the actual filter shape has been validated calculating the transfer function (*the* MATLAB function) by using the raw trace as the input and the filtered trace as the output. Therefore filter shapes shown in Fig. 5 are not calculated but real. All filters, even at lower frequencies (longer wavelengths) have the same perfect shape.

After filtering, signal belonging to defective sections has been removed, obtaining a set of shorter signals (Figure 6). RMS value of this set of signals has been computed; results are shown in Fig. 7.

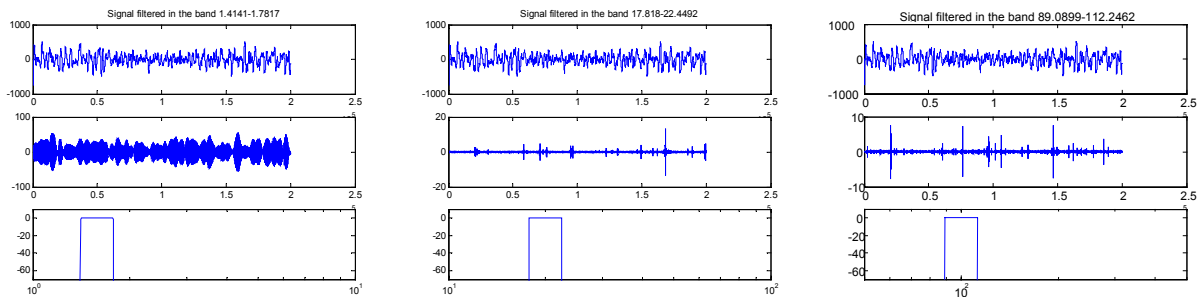


Figure 5. Left to right: examples of perfect filtering of Trace 2 for centre frequencies of 1.6 waves/m ( $\lambda=625$  mm), 20 waves/m ( $\lambda=50$  mm) and 100 waves/m ( $\lambda=10$  mm). Top to bottom: raw trace, filtered trace, filter shape (log x-axis showing 1 decade of spatial frequencies, y-axis in dB)

## 6. Conclusions

Long roughness measurements are easy and fast to perform and give many more information than short measurements. A new protocol to analyse them has been proposed, including a defect indicator function, a criterion for removing defective sections and the concept of perfect filtering. The application of the protocol is straightforward and can dramatically improved the quality of rail

roughness measurements. Future improvements are depicted, with particular reference to the update of current standards.

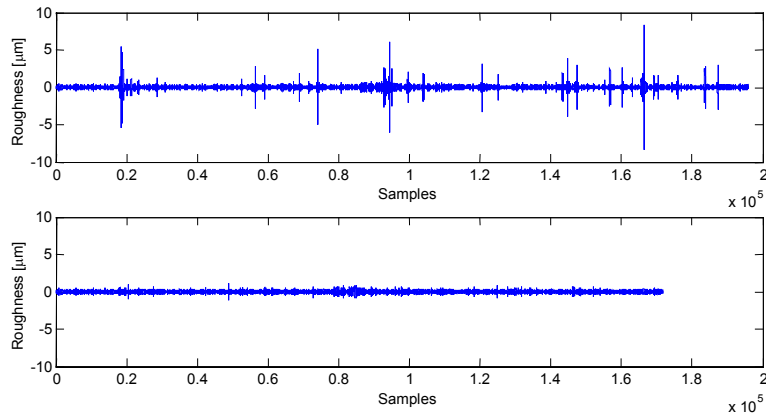


Figure 6. Above: roughness Trace 2 perfectly filtered at the 20 waves/m 1/3-octave spatial frequency ( $\lambda=50$  mm). Below: the same trace after removal of defective sections.

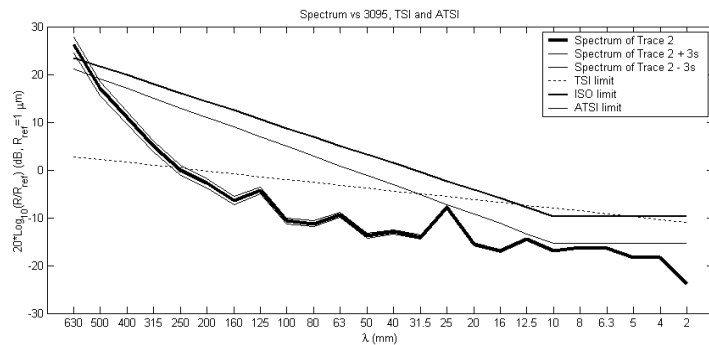


Figure 7. Roughness spectrum  $\pm 3\sigma$  of the entire track compared to limits of the standards. Statistical uncertainty is extremely low also at very long wavelengths. Also shown are the rail roughness limit spectra described in [1, 2, 3].

## References

- [1] International Organization for Standardization Draft ISO/DIS 3095:2001: Railway applications — Acoustics — Measurement of noise emitted by railbound vehicles, January 2001.
- [2] The Commission Of The European Communities: Technical specification for interoperability relating to the rolling stock subsystem, Official Journal of the European Communities, 12.9.2002.
- [3] P. Fodiman, Rail roughness characterisation. *Workshop on NOEMIE reference track*, Bruxelles 26.2.2003.
- [4] A. Bracciali, P. Folgarait, Rail Corrugation Measurements for Rolling Stock Type Testing and Noise Control, *Proceedings of the Techrail Workshop*, Paris, 14-15.03.2002 (on CD).
- [5] M. Norton, *Fundamentals of Noise and Vibrations Analysis for Engineers*, Cambridge University Press, 1991.
- [6] A. Bracciali, Roughness growth – A practical case, *Proceedings of the 8<sup>th</sup> International Workshop on Railway Noise*, Southampton, 7-11 September 2004.
- [7] P.E. Gautier, Influence of the rail roughness data processing – Benchmark. *Workshop on NOEMIE reference track*, Bruxelles 26.2.2003.
- [8] S. L. Grassie, M. J. Saxon, J. D. Smith, Measurement of longitudinal rail irregularities and criteria for acceptable grinding, *Journal of Sound and Vibration* 227 (1999), 949-964.
- [9] P. C. G. J. Dings *et al.* Report NSTO/97/9571011/005. Utrecht: NS Technisch Onderzoek. The measurement, analysis and presentation of wheel and rail roughness, 1997.
- [10] *Proceeding of the Workshop on Rail Roughness Measurements*, Utrecht, 31 May 1999
- [11] D.J. Thompson, On the relationship between wheel and rail surface roughness and rolling noise, *Journal of Sound and Vibration* 193 (1996), 149-160.
- [12] A. Bracciali, F. Piccioli, Experimental analysis of wheel noise emission as a function of the contact point location, *Journal of Sound and Vibration* 267 (2003), 469-483